

Dielectric properties and energy storage density in ZnO-doped $\text{Ba}_{0.3}\text{Sr}_{0.7}\text{TiO}_3$ ceramics

Guixia Dong^{*}, Shuwang Ma, Jun Du, Jiandong Cui

Advanced Electronic Materials Institute, General Research Institute for Nonferrous Metals, Beijing 100088, China

Received 25 July 2008; received in revised form 19 September 2008; accepted 12 November 2008

Available online 3 December 2008

Abstract

ZnO additions to $\text{Ba}_{0.3}\text{Sr}_{0.7}\text{TiO}_3$ ceramics have been studied in order to determine the role of this dopant on dielectric property and energy storage density development. The temperature and frequency dependences of dielectric constant, the breakdown strength, and the dielectric dissipation were measured. The dependence of dielectric constant to applied DC field was used to evaluate the energy storage densities. The crystalline structure and morphology were also investigated by XRD and SEM, respectively. Experimental results show that the stored energy density for the sample with 1.6 wt% ZnO addition is the highest among all the compositions. At 40 kV mm^{−1} electric field, its stored energy density can reach 3.9 J cm^{−3}. Moreover, the ceramic with this composition has higher dielectric constant and breakdown strength, lower loss and dependency characteristic of dielectric constant to applied electric field.

© 2008 Elsevier Ltd and Techna Group S.r.l. All rights reserved.

Keywords: Dielectric property; ZnO; Energy storage density; BST

1. Introduction

Multi-layer capacitors with a dielectric consisting essentially of barium titanate ceramic are a common component in many electronic systems. Because of the extremely high dielectric constant of this material at room temperature, the capacitance per unit volume that can be achieved is very large and the units are also robust and cheap. Under these conditions, the electric field strength applied to the dielectric layers of such capacitors is usually a small fraction of the breakdown electric field strength. It is found however, a capacitor of this type may not be well suited to applications requiring the maximum possible energy storage density [1]. In order to achieve high stored dielectric energy per unit volume, it is necessary for breakdown the electric field strength to be as high as possible. But when the applied voltage increases to a certain extent, the dielectric constant decreases markedly and the density of the stored energy that can be achieved is smaller than might be expected [1].

Empirical studies [2,3] have shown that the stored energy density in a ferroelectric ceramic at a given electric field strength is strongly dependent on composition. In 1996 [4,5], it has become possible to optimize composition and procedure based on the Devonshire model [6,7] of the behavior of ferroelectric materials. The optimization procedure leads to the selection of a composition that has a high value of crystal spontaneous polarization (P'_s) and a Curie temperature (T_c) well below the working temperature. At any given working field there is an optimal composition for $\text{Ba}_{1-x}\text{Sr}_x\text{TiO}_3$, the mole fraction of strontium increasing with increasing field strength. The development of these curves, giving the maximum attainable energy density for this family of materials, is approximately linear over the electric field range shown and has the form

$$U_{\max} \approx 0.08 E \quad (1)$$

when SI units are used [4].

According to Eq. (1), an energy density of about 4 J cm^{−3} should be attainable with this ceramic system at the breakdown field of about 50 kV mm^{−1}. If the breakdown field can be increased to 100 kV mm^{−1}, then an energy density of about 8 J cm^{−3} becomes attainable. However, the block ceramic is rarely totally densified, but defects (e.g. pores) are ineluctable. This situation may result in severe breakdown strength

^{*} Corresponding author. Tel.: +86 10 82241245.

E-mail address: dgxdgx01@163.com (G. Dong).

degradation and ultimately failure of the devices, which affects the capability for storing high density of energy. Generally, the breakdown strength of $\text{Ba}_{1-x}\text{Sr}_x\text{TiO}_3$ ceramics with 0.2–0.5 mm in thickness is about 20–50 kV mm⁻¹. Under this condition, the optimal Sr content lies in the range $x = 0.5$ –0.8 [4] for the maximum energy density.

This paper presents measurements of the dielectric parameters and the energy density of ZnO-doped $\text{Ba}_{0.3}\text{Sr}_{0.7}\text{TiO}_3$ ceramics. In view of the strong dependence of storage energy on electrical breakdown strengths, a comparison is made between the ZnO-doped and undoped $\text{Ba}_{0.3}\text{Sr}_{0.7}\text{TiO}_3$ ceramics.

2. Experimental procedure

Conventional ceramic fabrication processes were used to prepare the present ZnO-doped and undoped $\text{Ba}_{0.3}\text{Sr}_{0.7}\text{TiO}_3$ samples from analytical purity (above 99%) powders of BaCO_3 , SrCO_3 , TiO_2 , and ZnO. The BaCO_3 , SrCO_3 , and TiO_2 powders were mixed on a planetary ball-mill for 24 h with ethyl alcohol and agate balls in an agate pot. The volume ratio of agate balls to ethyl alcohol to powder is 6:2:1. The mixture was dried and calcined at 1100 °C for 4 h in air, then crushed into powder. The appropriate amount of ZnO was mixed with the $\text{Ba}_{0.3}\text{Sr}_{0.7}\text{TiO}_3$ powders by the same procedure outlined earlier. The powders then were pressed into disks of 20 mm in diameter and 4 mm thick under a cold isostatic pressure of 200 MPa after a uniaxial pressure of 4 MPa. No binder was used. The sintering of the green pellets was performed in air at 1200–1400 °C for 4 h, with heating and cooling rates of 100 °C/h.

The bulk density, porosity and shrinkage of the sintered samples were measured using ASTM (American Society for Testing and Materials) standards. Microstructures of the sintered samples were examined by scanning electron microscope (SEM, JSM-5610LV). X-ray diffraction (XRD, RIGAKU D/MAX-III A) with Cu-K radiation was used for phase identification. To determine the dielectric properties, the sintered samples were polished to a thickness of 0.2–0.5 mm and provided with electrodes of silver paste applied to both surfaces and fired at 650 °C for 0.2 h. The dielectric constant and loss were measured using a HP4294A at 40 Hz to 30 MHz from -40 °C to 40 °C. And the breakdown strength of samples with a thickness of 0.5 mm was measured on Trek Model 30/20 High-Voltage Power Amplifier. Stored energy of samples with a thickness of 0.2 mm was determined by measuring sample's capacitance with a small 500 Hz AC signal while superimposing an increasing DC bias on a TF Analyzer 2000 and then integrating the results. The measurements were made at room temperature. In all cases, measurements were continued until either the breakdown voltage of the specimen or the voltage capability of the measuring equipment was reached.

3. Results and discussion

3.1. Sintering and microstructure

The effect of ZnO content on the sintered $\text{Ba}_{0.3}\text{Sr}_{0.7}\text{TiO}_3$ is correlated with their densification, grain growth behavior, and

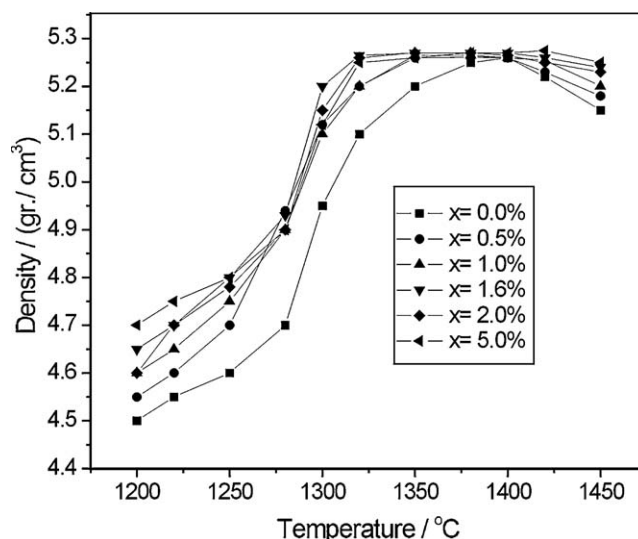


Fig. 1. Sintering temperature dependence of the density for $\text{Ba}_{0.3}\text{Sr}_{0.7}\text{TiO}_3 + x\%$ ZnO ceramics.

microstructure development. Fig. 1 shows the relationships among the compositions, sintering temperatures and densities of all samples.

ZnO-doped materials show a relative density (corresponding density) values as high as 99%, for sintering temperatures about 80 °C lower than that for the undoped $\text{Ba}_{0.3}\text{Sr}_{0.7}\text{TiO}_3$. High densities and homogeneous fine-grained microstructures were obtained in a wide range of sintering temperatures between 1320 °C and 1420 °C and when ZnO compositions between 0.5 wt% and 5.0 wt% (shown as Fig. 2). The Zn^{2+} cation has been considered as both an isovalent [8] and an acceptor [9] dopant in the BaTiO_3 lattice. Jaffe et al. [9] reported a solubility limit of 0.7 wt% ZnO at 1200 °C in BaTiO_3 . Swilam and Gadalla [10] found that ZnO addition above this limit leads to more densified BaTiO_3 ceramics, while the microstructure revealed the presence of a secondary liquid phase. Caballero et al. [11,12] observed coexistence of two phases in the microstructure of the 0.5 wt%-ZnO-doped sample and the second phase is ZnO. Roth et al. [13] also reported that BaTiO_3 and ZnO were the only crystalline phases detected in the system BaTiO_3 –ZnO below 1350 °C.

Fig. 3(a) shows the diffraction patterns of the undoped and ZnO-doped samples sintered at 1350 °C. ZnO peaks are clearly detected for the samples with the two highest ZnO contents (2 wt% and 5 wt%). However, the presence of ZnO grains in the samples with lower ZnO contents (<2.0 wt%) cannot be discerned in view of these results. Fig. 3(b) shows XRD patterns of 1.6 wt% ZnO powder blend into $\text{Ba}_{0.3}\text{Sr}_{0.7}\text{TiO}_3$ powder (mixed on a planetary ball-mill for 24 h with ethyl alcohol and agate balls in an agate pot), and ZnO can obviously be detected (curve 1 in Fig. 3(b)). But after sintering, the ZnO peaks vanished (curve 2 in Fig. 3(b)). It is possible that a certain number of Zn^{2+} as an isovalent or (and) an acceptor dopant diffused into $\text{Ba}_{0.3}\text{Sr}_{0.7}\text{TiO}_3$ lattice and the residual homogeneously distributes at grain boundaries during sintering. So it is very difficult to detect. Unlike reported by Caballero et al.

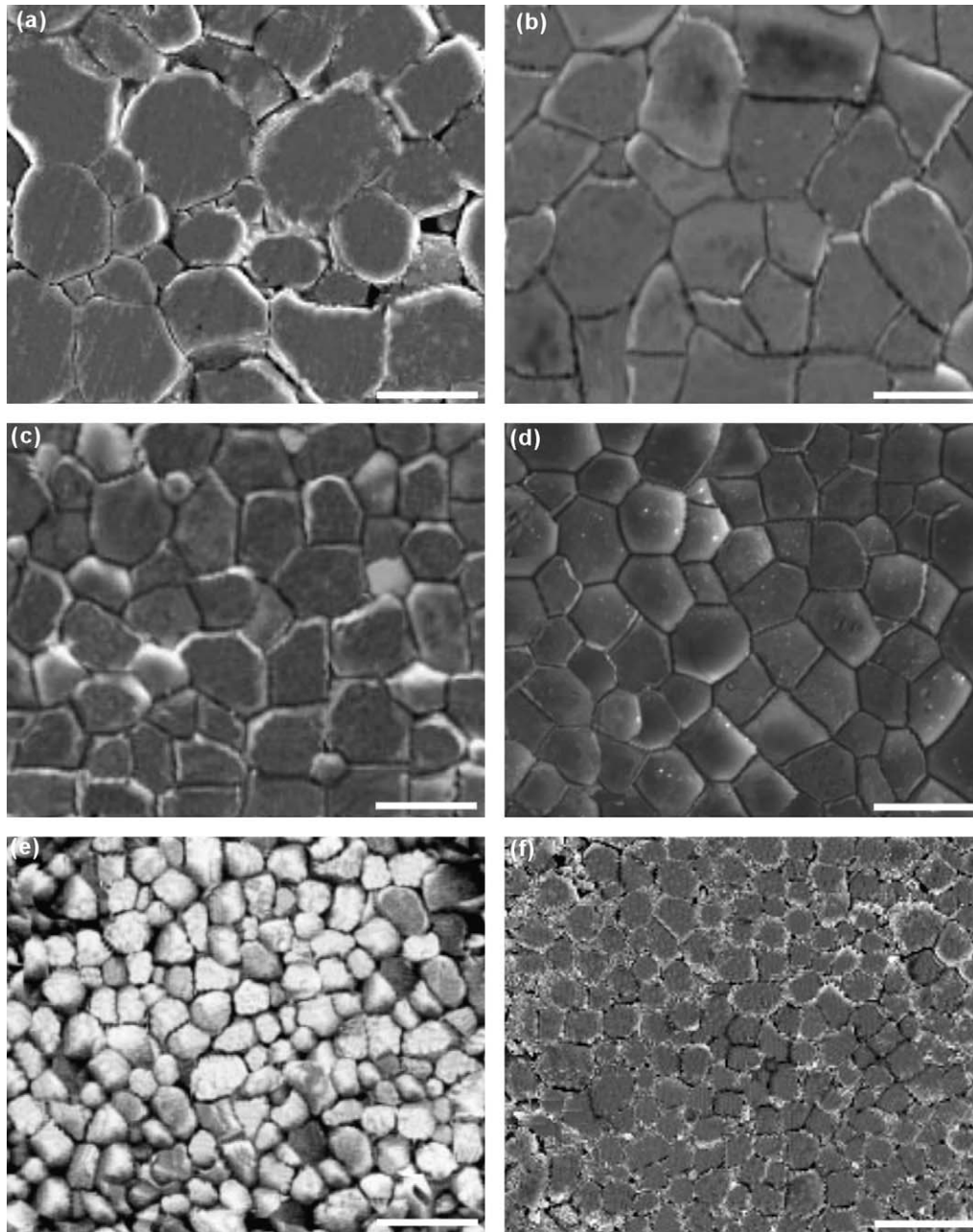


Fig. 2. SEM micrographs of samples sintered at 1350 °C. (a) $\text{Ba}_{0.3}\text{Sr}_{0.7}\text{TiO}_3$; (b) $\text{Ba}_{0.3}\text{Sr}_{0.7}\text{TiO}_3 + 0.5 \text{ wt\% ZnO}$; (c) $\text{Ba}_{0.3}\text{Sr}_{0.7}\text{TiO}_3 + 1.0 \text{ wt\% ZnO}$; (d) $\text{Ba}_{0.3}\text{Sr}_{0.7}\text{TiO}_3 + 1.6 \text{ wt\% ZnO}$; (e) $\text{Ba}_{0.3}\text{Sr}_{0.7}\text{TiO}_3 + 2 \text{ wt\% ZnO}$; (f) $\text{Ba}_{0.3}\text{Sr}_{0.7}\text{TiO}_3 + 5 \text{ wt\% ZnO}$. Scale bars are all 5 μm in length.

[11,12], obvious fine-grained microstructures are observed (Fig. 2) when ZnO content is above 0.5 wt%.

3.2. Dielectric properties and energy storage densities

Temperature dependence of the relative dielectric constant (ϵ_r) for $\text{Ba}_{0.3}\text{Sr}_{0.7}\text{TiO}_3$ specimens doped with ZnO is denoted in Fig. 4(a) and (b). In the temperature range between -40 °C and -10 °C, the dielectric constant slightly decreases with the increase in amount of ZnO. But at room temperature, it first increases with lower ZnO content because of higher density and smaller grains, and then decreases with more ZnO additives. Higher addition of ZnO leads to two-phase

microstructure, and hence the dielectric constant of the sample with the highest ZnO content (5 wt%) falls below the values measured for the rest samples. The dielectric losses for the samples doped with 0.5 wt%, 1.0 wt%, 1.6 wt% and 2 wt% ZnO, respectively, are lower than that of the undoped one. Nevertheless, this cannot be due to the density, since all the samples sintered at 1350 °C showed high density (relative density greater than 98%). It is considered that ZnO additions may cause a lower conductivity in the material [11,12]. Fig. 4(c) shows the frequency dependence of the dielectric constants of the ZnO-doped samples. The relationships between dielectric constant and composition also can be clearly observed from Fig. 4(c).

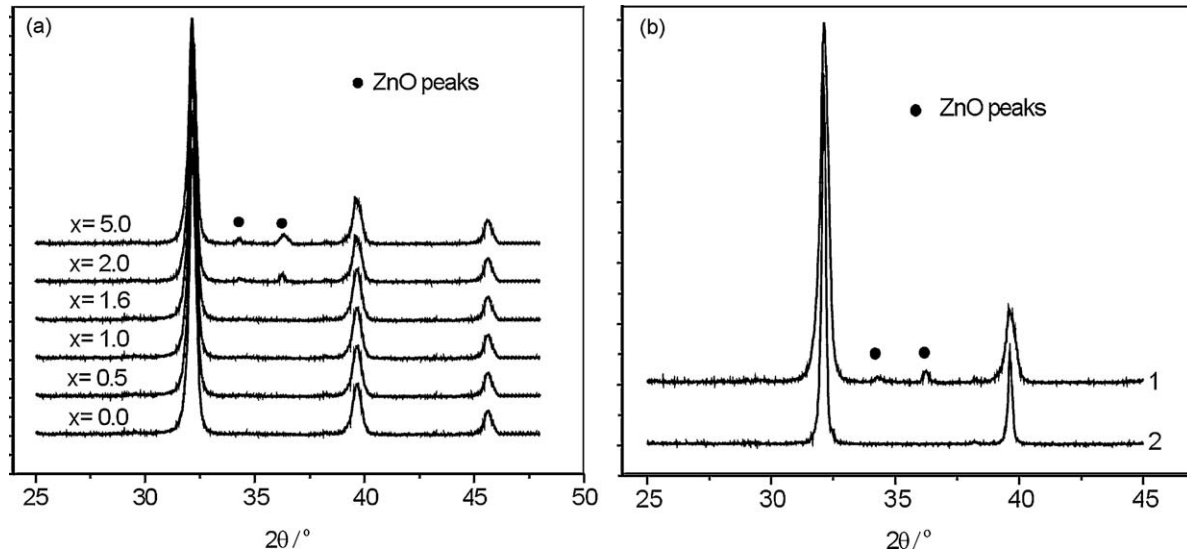


Fig. 3. XRD patterns: (a) $\text{Ba}_{0.3}\text{Sr}_{0.7}\text{TiO}_3 + x \text{ wt\% ZnO}$ samples sintered at 1350 °C; (b) $\text{Ba}_{0.3}\text{Sr}_{0.7}\text{TiO}_3$ powder mechanically blended with 1.6 wt% ZnO powder (curve 1) and $\text{Ba}_{0.3}\text{Sr}_{0.7}\text{TiO}_3 + 1.6 \text{ wt\% ZnO}$ sintered at 1350 °C (curve 2).

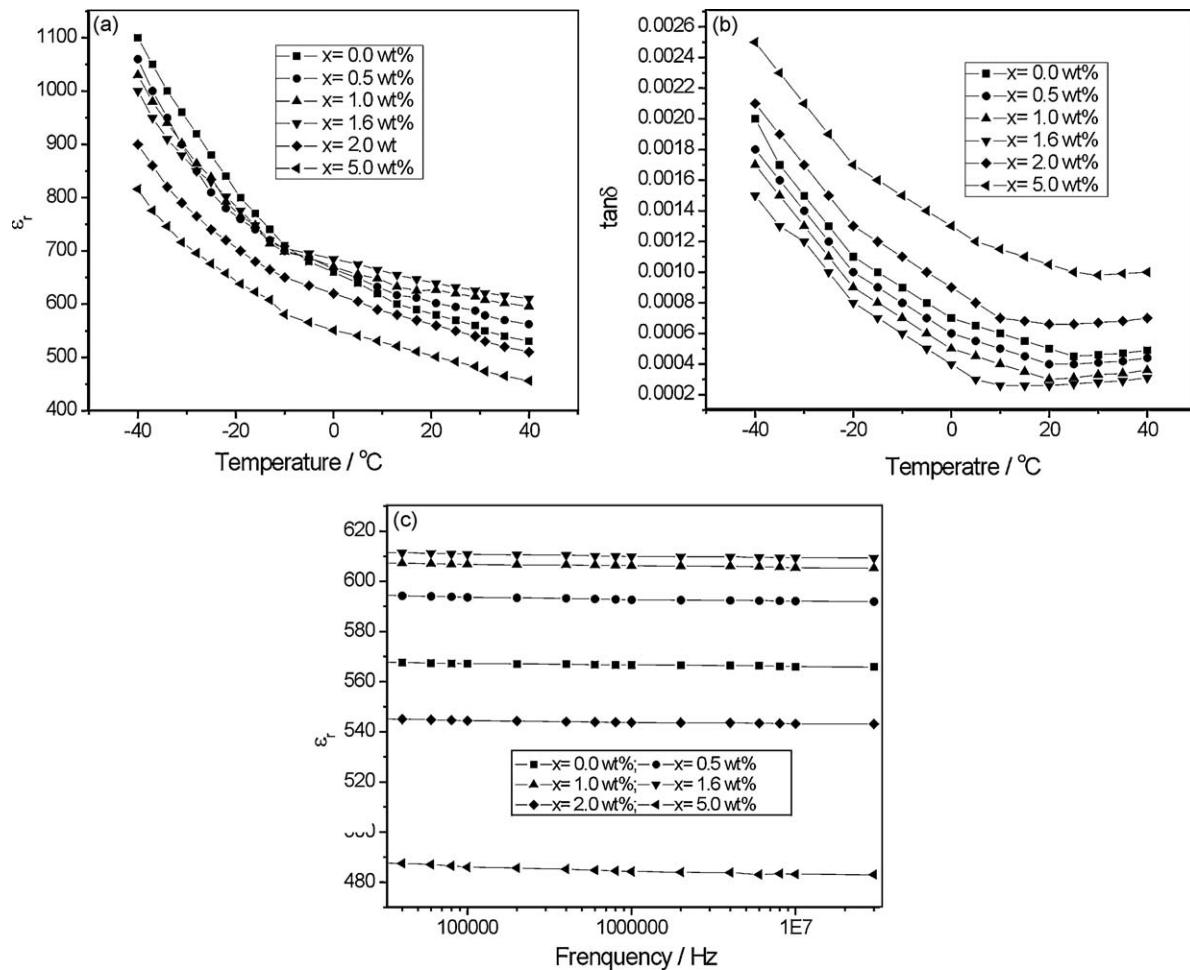


Fig. 4. Dielectric properties of $\text{Ba}_{0.3}\text{Sr}_{0.7}\text{TiO}_3 + x \text{ wt\% ZnO}$ ceramics sintered at 1350 °C. (a) The temperature dependence of dielectric constant; (b) temperature dependence of dielectric loss; (c) frequency dependence of dielectric constant. The measurement frequency was 1 kHz for (a) and (b).

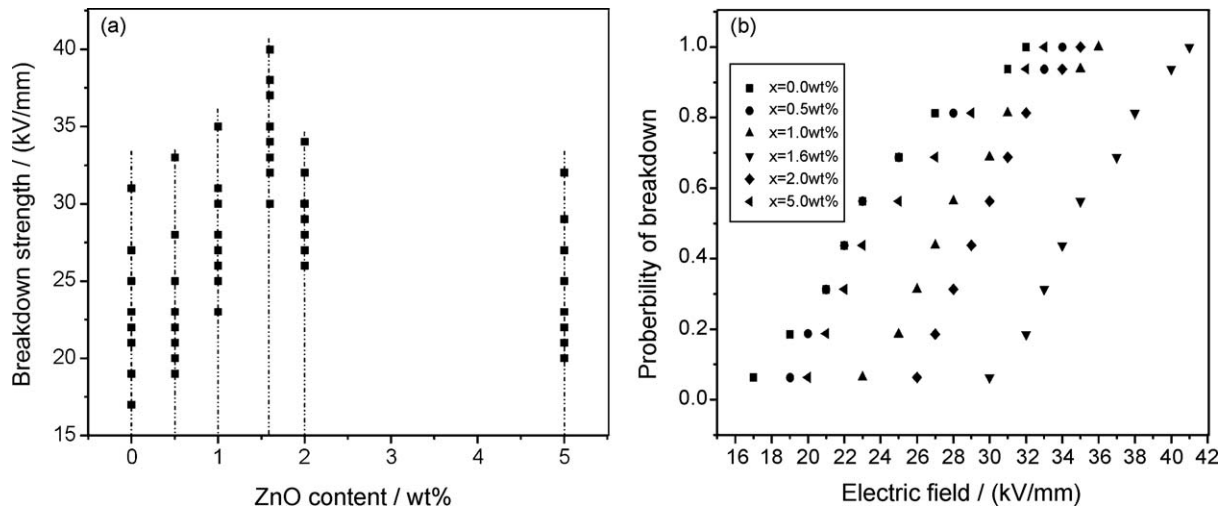


Fig. 5. Breakdown strength (a) and breakdown statistics plotted as a Weibull distribution (b) of $\text{Ba}_{0.3}\text{Sr}_{0.7}\text{TiO}_3 + x \text{ wt\% ZnO}$ samples sintered at 1350°C .

The relationships between ZnO content in samples and breakdown strength are illustrated in Fig. 5(a). The number of samples in the breakdown strength test for each ZnO content is 8. It can be seen from Fig. 5(a) that the measured value was scattered. This is because that the electrical strength of ceramics is likely dependent on the statistical distribution of defects in the material. For this reason, the Weibull distribution was used to describe the results of Fig. 5(a) as Fig. 5(b). Clearly, the breakdown strength for 1.6 wt% ZnO content is much higher than others. Reasonably, electric strength depends markedly on material homogeneity. A ceramic is rarely homogeneous, a common inhomogeneity being porosity. There is robust evidence to show that breakdown can be initiated at pores and that the occurrence of gas discharges within pores is an important factor [14], although how discharges within pores lead to total breakdown of the dielectric has been a matter of debate. It may result from the propagation of a discharge ‘streamer’ through the ceramic, possibly progressing from pore to pore and encouraged by the

increased electric stress to which the material between discharging pores is subjected and perhaps also by enhanced stress in the material close to a discharging pore [14]. Clearly the larger in size and in number the pores are, the more easily the ceramic breaks down. Finer grain and higher density microstructure obtained by adding ZnO into $\text{Ba}_{0.3}\text{Sr}_{0.7}\text{TiO}_3$ ceramic (see Fig. 2) eliminates the pore number and size and lengthens the grain boundary thereby reducing the probability of occurrence of a critical defect, making the progressing of discharge ‘streamer’ more curved and long at the given electric stress, and results in an increase in breakdown strength. When the addition of ZnO increases to some extent (e.g. above 2 wt%), the breakdown strength of the ceramic will decrease. This is because the phase boundaries between ZnO with a hexahedral closely packed structure and ferroelectric phase with a perovskite-type structure increase. Moreover, ZnO phase has a voltage-dependent resistance, i.e. it offers a high resistance at low voltages and a low resistance at high voltages, and therefore it is likely unfavorable for $\text{Ba}_{0.3}\text{Sr}_{0.7}\text{TiO}_3$

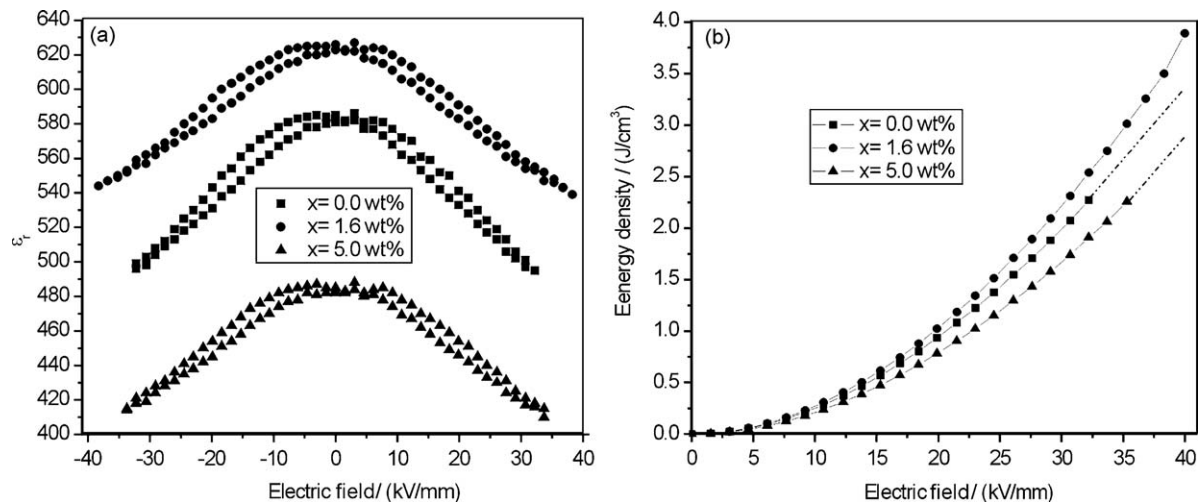


Fig. 6. Electric field dependence of dielectric constant (a) and energy density (b) for $\text{Ba}_{0.3}\text{Sr}_{0.7}\text{TiO}_3 + x \text{ wt\% ZnO}$ samples sintered at 1350°C .

ceramic doped with high ZnO contents (above 2 wt%) to obtain high breakdown strength.

The DC field dependence of ϵ_r for the studied samples is shown in Fig. 6(a). Applying DC field reduces the dielectric constant. The dielectric constant for the undoped sample has the highest electric field dependence, with a dielectric constant tunability of 16.1% under an electric field of 31 kV mm⁻¹ (i.e. $(\epsilon_{r0} - \epsilon_{r31})/\epsilon_{r0} = 16.1\%$; ϵ_{r0} and ϵ_{r31} are the dielectric constants of ceramic under electric fields of 0 kV mm⁻¹ and 31 kV mm⁻¹, respectively). It could be explained that the grain size and the internal stress among grains influence the dielectric properties. The larger grains have smaller stress. So the dielectric constant is liable to change by applied electric field. Fig. 6(b) shows the dependence of stored energy density on electric field strength for samples with three compositions (0 wt%, 1.6 wt% and 5 wt% ZnO). The Ba_{0.3}Sr_{0.7}TiO₃ ceramic doped with 1.6 wt% ZnO has a higher dielectric constant, higher breakdown strength and lower dependency of dielectric constant to electric field (the dielectric constant tunability is 13.6% under applied electric field 31 kV mm⁻¹), and the stored energy density for the ceramic with this composition represents the best result obtained from ZnO-doped and undoped Ba_{0.3}Sr_{0.7}TiO₃ ceramics. At 40 kV mm⁻¹ electric field (the voltage capability of the measuring equipment was reached), its stored energy density can reach 3.9 J cm⁻³. This value is greater than the calculated result from Eq. (1) that was predicted by the Devonshire model based on pure or undoped Ba_{1-x}Sr_xTiO₃ ceramics. For the undoped Ba_{0.3}Sr_{0.7}TiO₃ ceramic, the maximum value of the storage energy density, obtained at an electric field of 31 kV mm⁻¹ (the breakdown strength of this ceramic), is 2.25 J cm⁻³, which shows quite good agreement with that calculated from Eq. (1). The Ba_{0.3}Sr_{0.7}TiO₃ ceramic containing the highest ZnO (5 wt%; Fig. 6(b)) has a maximum stored energy density of 2.53 J cm⁻³, gotten at the breakdown strength (34 kV mm⁻¹). This value is also less than that calculated from Eq. (1), indicating that much more ZnO additions to the ceramic are unfavorable for improving the storage energy density. This is likely because when ZnO addition is more than a certain extent (e.g. 1.6 wt% ZnO), it leads to a decrease of the dielectric constant and breakdown strength of the ceramic, thereby resulting in lower stored energy density. The above results can be explained from following expression for the energy storage density of a material:

$$U = \frac{1}{2} \epsilon_0 \epsilon_{rE} E^2 \quad (2)$$

here U is the energy storage density, ϵ_0 is the dielectric constant in vacuum, and ϵ_{rE} is the relative dielectric constant at an electric field strength (E).

From Eq. (2), it can be deduced that the higher the electric field (E) and the primary dielectric constant (when $E = 0$) and the weaker the dependency of the dielectric constant on the electric field strength, the higher the energy storage density (U). As aforementioned, the ceramic Ba_{0.3}Sr_{0.7}TiO₃ doped with 1.6% ZnO has a higher primary dielectric constant and a higher breakdown strength (it is not breakdown yet when

the voltage reaches 40 kV mm⁻¹) with a weaker dielectric dependency on electric field strength, and thus this material can obtain higher energy storage density (higher than 3.9 J cm⁻³). In contrast, the ZnO-undoped sample, with a lower primary dielectric constant, a lower breakdown strength (~ 31 kV mm⁻¹) and a stronger dependency of dielectric constant on electric field strength, has a lower energy storage density (the maximum energy storage density is only 2.25 J mm⁻³). For the samples with relatively high ZnO contents (e.g. 5 wt% ZnO), although they have relatively weak field strength dependency of the dielectric constants (the dielectric constant tunability for 5 wt% ZnO sample is $\sim 13.4\%$), both their primary dielectric constant and breakdown strengths (~ 34 kV mm⁻¹) are relatively low, and therefore it is unsuitable for these ceramics to obtain high energy storage density (the maximum value is only 2.26 J cm⁻³).

From present study results, the highest energy storage density (above 3.9 J cm⁻³) were obtained from the ceramic Ba_{0.3}Sr_{0.7}TiO₃ doped with 1.6% ZnO; the maximum storage density for the ZnO-undoped sample is only 2.25 J mm⁻³. As a consequence, addition of a certain amount of ZnO to Ba_{0.3}Sr_{0.7}TiO₃ ceramic has a significant effect on increasing its energy storage density.

4. Conclusions

Addition of ZnO can make Ba_{0.3}Sr_{0.7}TiO₃ ceramic blocks densified easily and have fine-grained microstructures. The decrease of the loss tangent value and the increase of the dielectric constant and breakdown strength reveal that ZnO doping could be very interesting for Ba_{1-x}Sr_xTiO₃ based dielectric ceramics for high quality capacitors. The dielectric energy storage densities of ZnO-doped and undoped Ba_{0.3}Sr_{0.7}TiO₃ ceramics have been investigated and it has been found that the stored energy density for the ceramic with 1.6 wt% ZnO addition is the highest among all the compositions. Correspondingly, this composition has higher dielectric constant and breakdown strength, and lower dependency characteristic of dielectric constant to applied electric field. It seems that these characteristics originate from the fine grains, high block density, and an increase of the resistivity of the ZnO-doped material.

References

- [1] B.W. Ricketts, G. Triani, A.D. Hilton, Dielectric energy storage densities in Ba_{1-x}Sr_xTi_{1-y}Zr_yO₃ ceramics, *Journal of Material Science: Materials in Electronics* 11 (6) (2000) 513–517.
- [2] I. Burn, D.M. Smyth, Energy storage in ceramic dielectrics, *Journal of Material Science* 7 (3) (1972) 339–343.
- [3] G.R. Love, Sprague Technical 87-4, American Ceramic Society Spring Meeting, Pittsburgh, April, 1987.
- [4] N.H. Fletcher, A.D. Hilton, B.W. Ricketts, Optimization of energy storage density in ceramic capacitors, *Journal of Physics D: Applied Physics* 29 (1) (1996) 253–258.
- [5] A.D. Hilton, B.W. Ricketts, Dielectric properties of Ba_{1-x}Sr_xTiO₃ ceramics, *Journal of Physics D: Applied Physics* 29 (5) (1996) 1321–1325.

- [6] A.F. Devonshire, Theory of barium titanate. Part I, *Philosophical Magazine* 40 (309) (1949) 1040–1063.
- [7] A.F. Devonshire, Theory of ferroelectrics, *Advances in Physics* 3 (10) (1954) 85–130.
- [8] P. Baxter, N.J. Hellicar, B. Lewis, Effect of additives of limited solid solution on ferroelectric properties of barium titanate ceramics, *Journal of the American Ceramic Society* 42 (10) (1959) 465–470.
- [9] B. Jaffe, W.R. Cook, H. Jaffe, *Piezoelectric Ceramics*, Academic Press, New York, 1971.
- [10] M.N. Swillam, A.M. Gadalla, Effect of additions on the sinterability of barium titanate, *Journal of the British Ceramic Society* 74 (5) (1975) 165–169.
- [11] A.C. Caballero, J.F. Fernandez, C. Moure, P. Duran, ZnO-doped BaTiO₃: microstructure and electrical properties, *Journal of the European Ceramic Society* 17 (4) (1997) 513–523.
- [12] A.C. Caballero, J.F. Fernández, C. Moure, P. Durán, Y. Chiang, Grain growth control and dopant distribution in ZnO-doped BaTiO₃, *Journal of American Ceramic Society* 81 (4) (1998) 939–944.
- [13] R.S. Roth, C.J. Rawn, C.G. Lindsay, W. Won-Ng, Phase equilibria and crystal chemistry of the binary and ternary barium polytitanates and crystallography of the barium zinc polytitanates, *Journal of Solid State Chemistry* 104 (1) (1993) 99–118.
- [14] A.J. Moulson, J.M. Herbert, *Electroceramics: Materials Properties Applications*, second ed., John Wiley & Sons Ltd., Chichester, 2003.